

1 **Isolation and functional characterization of hemp seed protein-derived short-**
2 **and medium-chain peptide mixtures with multifunctional properties for**
3 **metabolic syndrome prevention**
4
5

6 Andrea Cerrato^{a,1}, Carmen Lammi^{b,*,1,2}, Anna Laura Capriotti^{a,*,2}, Carlotta Bollati^b, Chiara Cavaliere^a,
7 Carmela Maria Montone^a, Martina Bartolomei^b, Giovanna Boschin^b, Jianqiang Li^b, Susy Piovesana^a,
8 Anna Arnoldi^b, Aldo Laganà^a

9
10 ^a Department of Chemistry, Sapienza University of Rome, Piazzale Aldo Moro 5, 00185 Rome,
11 Italy

12 ^b Department of Pharmaceutical Sciences, University of Milan, Via Mangiagalli 25, 20133 Milan,
13 Italy

14
15 ¹ These authors equally contributed to this work

16 ² These authors equally contributed to this work
17

18 ***Corresponding authors:** Carmen Lammi Department of Pharmaceutical Sciences, University of
19 Milan Via Mangiagalli 25, 20133 Milan, Italy E-mail: carmen.lammi@unimi.it

20 Anna Laura Capriotti, Department of Chemistry, Università di Roma “La Sapienza” Piazzale Aldo Moro 5,
21 00185 Rome, Italy E-mail: annalaura.capriotti@uniroma1.it

22
23
24
25 **Abbreviations**

26 ACE: angiotensin converting enzyme

27 ANOVA: analysis of variance

28 AP: apical

29 BCA: Bicinchoninic Acid Protein Assay

30 BL: basolateral

31 DPP-IV: dipeptidyl peptidase IV
32 DPPH: 2,2-Diphenyl-1-picrylhydrazyl
33 EFSA: European Food Safety Authority
34 FRAP: Ferric Reducing Antioxidant Power
35 GCB: graphitized carbon black
36 HMGCoAR: 3-hydroxy-3-methyl-glutaryl-coenzyme A reductase
37 LDL: low-density lipoprotein
38 LDLR: low-density lipoprotein receptor pathway
39 M: medium-chain peptide mixture of the hemp seed hydrolysate
40 MetS: Metabolic Syndrome
41 MTT: 3-(4,5-dimethylthiazol-2-yl)-2,5-diphenyltetrazolium bromide
42 PCSK9: Proprotein convertase subtilisin/kexin type 9
43 PepT1: peptide transport 1
44 RYR: red yeast rice
45 S: short-chain peptide mixture of the hemp seed hydrolysate
46 SDC: sodium deoxycholate
47 SEC: size exclusion chromatography
48 T: total hemp seed hydrolysate
49 TFA: trifluoroacetic acid
50 UFM: ultrafiltration membrane
51 UHPLC-HRMS: ultra-high-performance liquid chromatography - high-resolution mass
52 spectrometry

53

54

55

56

57 **Abstract**

58

59 This study aims to obtain a valuable mixture of short-chain peptides from hempseed as a new
60 ingredient for developing nutraceutical and functional foods useful for preventing metabolic
61 syndrome that represents the major cause of death globally.

62 A dedicated analytical platform based on a purification step by size exclusion chromatography or
63 ultrafiltration membrane and high-resolution mass spectrometry was developed to isolate and

64 comprehensively characterize short-chain peptides leading to the identification of more than 500
65 short-chain peptides. Our results indicated that the short-chain peptide mixture was about three times
66 more active than the medium-chain peptide mixture and total hydrolysate with respect to measured
67 inhibition of the angiotensin-converting enzyme. The short-chain peptide mixture was also two times
68 more active as a dipeptidyl peptidase IV, and two-fold more active on the cholesterol metabolism
69 pathway through the modulation of low-density lipoprotein receptor.

70

71 **Keywords:** peptidomics, size-exclusion chromatography, LC-HRMS, ACE, DPP-IV, HMGCoAR

72

73

74

75 **1. Introduction**

76

77 Metabolic syndrome (MetS) comprises a cluster of metabolic abnormalities, including accumulation
78 of lipids, insulin resistance, and chronic inflammation, leading to three main long-term medical
79 conditions, i.e., type II diabetes, ischemic stroke, and cardiovascular diseases, which represent the
80 first cause of death globally (Saklayen, 2018). The current management to address MetS-related
81 abnormalities includes adopting a healthy lifestyle and following a long-term medication regimen,
82 often involving administering several expensive drugs, which is challenging for patients (Lillich et
83 al., 2021).

84 Nowadays, research and development in the nutraceutical field offer the opportunity to prepare
85 patented proprietary combinations of chemically well-defined nutraceuticals to improve specific
86 health issues as support to conventional drug treatments. Based on natural bioactive compounds,
87 preventive and therapeutic methods are free from significant side effects and could represent a proper
88 adjuvant treatment to reduce hospitalization and health costs and improve the quality of life of MetS
89 patients (Santini & Novellino, 2017).

90 In this context, the administration of red yeast rice (RYR) extract, containing Monacolin K, represents
91 an effective strategy for promoting vascular and metabolic health (Yuan et al., 2022). On the other
92 side, the natural compound berberine can reduce cholesterolemia by increasing low-density
93 lipoprotein (LDL) cholesterol receptors on the liver cell surface and inhibiting triglycerides
94 biosynthesis by activating the adenosine monophosphate-activated proteokinase (Brusq et al., 2006).

95 In addition, berberine modulates the proprotein convertase subtilisin/kexin type 9 (PCSK9) gene
96 expression by acting on the expression of its selective transcription factor HNF1-alpha, improving
97 LDL receptor pathway (LDLR) stability (Dong et al., 2015). These considerations suggest that the
98 combined administration of RYR and berberine may provide a broader range of health protection
99 than the one afforded by prescribed statin therapy (McCarty et al., 2015). Despite the wide use of this
100 product, due to the presence of monacolin K (MonK, the same compound sold with the commercial

101 name of lovastatin), RYR possesses specific adverse effects that are typical of statins, such as liver
102 damage and muscle disorders (myopathy) (Mazzanti et al., 2017). Therefore, it is necessary to find
103 new active ingredients to replace RYR in the formulation of dietary supplements to prevent
104 hypercholesterolemia and cardiovascular diseases. Indeed, the European Food Safety Authority
105 (EFSA) has just delivered a scientific opinion on the safety of monacolins, the active ingredients from
106 RYR, and provided advice on the dietary intake of monacolins that does not give rise to concerns
107 about harmful effects. Exposure to MonK does not lead to severe adverse effects on the
108 musculoskeletal system, including rhabdomyolysis, and on the liver only at doses inferior to 3
109 mg/day. It is important to underline that in most commercial food supplements, the current MonK
110 dosage is 10 mg/day, a level considered by the panel as a significant safety concern (EFSA Panel on
111 Food Additives and Nutrient Sources added to Food 2018).

112 Considering all mentioned issues, discovering alternative nutraceutical products is a priority for
113 the food and nutrition industry. Among the great diversity of functional phytochemicals, bioactive
114 peptides have stood out as functional compounds due to their ability to reach the bloodstream and
115 exert biological activity (Pérez-Gregorio et al., 2020). More recently, short-chain peptides (i.e.,
116 peptides with 2-4 amino acid long sequences) were becoming particularly interesting and showed
117 advantages over longer peptide sequences; in particular, short-chain peptides have low cytotoxicity
118 and the ability to maintain their biological properties unaltered upon absorption, as they are not
119 subject to in-vivo transformation (Webb et al., 1992). In addition, multifunctional peptides represent
120 a new concept in the field (Lammi, Aiello, et al., 2019). In particular, this definition indicates the
121 peptides that have the capacity to impart more than one physiological outcome by affecting different
122 targets. In the case of food hydrolysates, the multifunctionality could be due to: a) the presence of
123 peptides that have different bioactivities even though they are monofunctional; b) the existence of
124 truly multifunctional peptides; c) to synergistic or interaction effects between different peptides
125 Recently, it has been demonstrated that protein hydrolysates derived from the hydrolysis of *Chlorella*
126 *pyrenoidosa* and *Spirulina (Arthrospira platensis)* proteins with pepsin inhibit both dipeptidyl

127 peptidase IV (DPP-IV) and angiotensin-converting enzyme (ACE), respectively (Aiello et al., 2019;
128 Li et al., 2021).

129 In this work, an analytical platform based on high-throughput techniques was developed to purify and
130 tentatively identify short peptide sequences produced from hemp seed proteins. Hemp seed samples
131 were selected since they possess high nutritional content (about 30% proteins). Recent research based
132 on *in-vitro* or *in-vivo* experiments has shown that hydrolysates obtained from hemp seed proteins
133 possess several biological activities (Aguchem et al., 2022). More in detail, size exclusion
134 chromatography (SEC) and membrane ultrafiltration (UFM) with a molecular cut-off < 1 kDa were
135 tested to maximize the isolation yield of short-chain peptides, considering issues due to the wide
136 range of polarity of these molecules and the complexity of the hempseed hydrolysates.

137 The composition of the purified extracts was investigated by a suspect screening untargeted
138 metabolomics approach based on ultra-high-performance liquid chromatography coupled to high-
139 resolution mass spectrometry (UHPLC-HRMS) and bioinformatics, devised explicitly for the
140 profiling of short-chain peptides. The biological activity associated with the prepared hydrolysates
141 was tested for the specific needs of MetS improvement. In particular, **the anti-DPP-IV, anti- ACE,
142 and anti-HMGCoAR, and antioxidant activities were investigated**. Initially, *in vitro* studies were
143 carried out to measure the inhibitory activity of the hydrolysates on relevant enzymes such as ACE,
144 DPP-IV, and HMGCoAR. The cholesterol-lowering activity of hempseed peptides was characterized
145 using HepG2 cells to assess their effects on the cholesterol metabolism pathway. Afterward, the
146 human intestinal Caco-2 cells were employed to assess the effects of the hydrolysates on the DPP-IV
147 activity modulation. Then, *ex vivo* experiments were performed using the human serum to evaluate
148 the effect of hempseed short-chain peptide mixture on circulating DPP-IV. The bioactivity of food
149 peptides depends not only on their biological effects but also on bioavailability at the intestinal level,
150 reaching intact the organs where they can exert health-promoting activity (Lammi, Aiello, et al.,
151 2019). In general, short-chain peptide mixture tend to be absorbed faster than medium- and/or long-
152 chain ones by enterocytes (Lammi, Aiello, et al., 2019). Hence, differentiated Caco-2 cells were used

153 as a reliable model for assessing the ability of short-chain peptide mixture (S) to be transported at the
154 intestinal level, addressing delicate issues related to their stability and bioavailability.

155

156 **2. Materials and methods**

157

158 **2.1 Protein extraction and digestion**

159 Hemp flour, obtained from ground seeds of the hemp variety Futura 75, was purchased in a local
160 market. The protein content declared on the label was 40%.

161 Fifty mg of hemp flour was extracted with 2 mL of a buffer containing 50 mmol/L of Tris-HCl (pH
162 8.5) and 2% (w/v) of sodium deoxycholate (SDC). The sample was incubated on ice for 1 h with
163 intermittent vortexing (1 min) every 15 minutes. After this step, samples were placed in an ultrasonic
164 bath for 1 h; the entire cycle was repeated twice, and, finally, the insoluble material was removed by
165 centrifugation at room temperature for 20 min at $20\,000 \times g$. The extracted proteins were quantified
166 by Bicinchoninic Acid Protein Assay (BCA) using bovine serum albumin as standard as previously
167 described (Walker, 1996).

168 After quantification, hemp protein was hydrolysed by Alcalase®, as previously described (Montone
169 et al., 2018). Briefly, a 15 mg protein aliquot was diluted with 50 mmol L⁻¹ Tris-HCl (pH 8.8) to
170 obtain a final urea concentration of 0.8 mol/L. Alcalase was added (1:10, enzyme: protein ratio), and
171 samples were incubated at 60 °C for 4 h. Enzymatic hydrolysis was quenched by decreasing the pH
172 to 2 with trifluoroacetic acid (TFA). The hydrolysed sample was centrifuged for 10 min at 20 000 x
173 g at room temperature to remove SDC that precipitates in acid environment. The resulting peptide
174 mixture was stored at -20 °C until analysis. More in details, following this procedure, three
175 independent hydrolysates T were produced. The peptide concentration was determined by GoA assay,
176 according to Lammi et al., (Lammi et al., 2016), based on chelating the peptide bonds by Cu (II) in
177 alkaline media and controlling the change of absorbance at 330 nm. In brief, the reagent contained
178 0.6 M sodium citrate, 0.9 M sodium carbonate, and 0.07 M copper sulfate, 2.4 M NaOH at pH 10.6.
179 A solution containing X µL peptide mixture, (500 - X) µL water, 500 µL 6% (w/w) NaOH in water,

180 and 50 μ L active reagent was prepared. The optical density of the solution was measured at 330 nm.
181 A sterile solution of peptone (10 mg/mL) in water was used as standard for the calibration curve.

182

183 **2.2 Evaluation of the degree of hydrolysis (DH)**

184 The DH was determined by the o-phthalaldehyde (OPA) assay, according to Nielsen et al., 2001
185 (<https://doi.org/10.1111/j.1365-2621.2001.tb04614.x>) with certain modifications. This assay is based
186 on the formation of an adduct between the α -amino groups of peptides and the OPA reagent. 200 μ L
187 of OPA reagent were mixed with 26.6 μ L of hydrolysates, the absorbance was assessed at 340 nm
188 using the Synergy H1 fluorescent reader (Biotek, Bad Friedrichshall, Germany) after 1.5 min of
189 incubation at 25 $^{\circ}$ C.

190 **2.3 Peptide separation**

191 The Alcalase hydrolysate was subjected to peptide separation using two different protocols, namely
192 SEC and UFM systems.

193

194 **2.3.1 Size exclusion chromatography**

195 The total hydrolysate was subjected to peptide separation using a BIOBASIC SEC 120, 5 μ m, 150 x
196 7.8 mm (Thermo, Waltham, Massachusetts, USA) connected to a Shimadzu Prominence LC-20A
197 system, including a CBM-20A controller, two LC-20 AP preparative pumps and a DGU-20A3R
198 online degasser. An SPD-20A UV with a preparative cell (0.5 mm) was used as a detector and was
199 set at 214nm. An FRC-10A Shimadzu was employed as an auto collector. Data acquisition was
200 performed by the LabSolution version 5.53 software (Shimadzu, Kyoto, Japan).

201 The sample was eluted in isocratic with a flow rate of 1 mL/min using ddH₂O/TFA (99.9/0.1, v/v).

202 Two fractions were collected, as shown in Figure 1S. The fraction collected from 1 to 5 min contained
203 medium-sized peptides, while the fraction collected from 6 to 10 min contained short peptides.

204 The dry weight of the mixture was 14.7 mg (98% w/w).

205 **2.3.2 Ultrafiltration**

206 The total hydrolysate was subjected to Ultrafiltration Discs, 1 kDa NMW (Ultracel®) regenerated
207 cellulose, 44.5 mm in diameter. The filter was initially pre-treated and rehydrated in H₂O for 1 h to
208 remove impurities from the manufacturing process or additives used for stabilization. After that, the
209 membranes were washed three times with Milli-Q water and stored before use. Freshly pre-treated
210 membranes were used in all experiments unless indicated otherwise.

211 Then, the filter was rinsed three times with 3 mL of MeOH, once with 1 mL of deionized H₂O/TFA
212 (99.9/0.1, v/v), and stored before use. Freshly pre-treated membranes were used in all experiments
213 unless indicated otherwise. Fifteen mg of the total hydrolysate was transferred to the membrane and
214 filtered by Millipore classic glass filter holder. The filtrate, containing short-chain peptide mixture,
215 was recovered and dried. The dry weight of the purified mixture was 6 mg (40% w/w).

216

217 **2.4 Analysis of medium-chain peptide mixture by nano-high performance liquid** 218 **chromatography-MS/MS**

219 Medium-chain peptide mixture obtained from SEC chromatography were analyzed by nano HPLC
220 on an Ultimate 3000 (Thermo Fisher Scientific, Bremen, Germany) coupled to an Orbitrap Elite mass
221 spectrometer (Thermo Fisher Scientific). According to the manufacturer's instructions, the mass
222 spectrometer was calibrated once a week using the Pierce LTQ Velos ESI Positive Ion Calibration
223 Solution (Thermo Fisher Scientific). Mass accuracy was <1.5 ppm without lock-mass. Medium-chain
224 peptide mixture was analyzed as previously described (Cerrato, Capriotti, et al., 2020), with some
225 modifications. Twenty µL were online preconcentrated on a µ-precolumn (Thermo Fisher Scientific,
226 300 µm i.d. × 5 mm Acclaim PepMap 100 C18, 5 µm particle size, 100 Å pore size) at 10 µL/min
227 flow rate of a premixed mobile phase H₂O/ACN 98:2 (v/v) containing 0.1% (v/v) TFA. Then,
228 samples were separated on an EASY-Spray column (Thermo Fisher Scientific) 15 cm × 75 µm i.d.
229 PepMap C18, 3 µm particles, 100 Å pore size operated at 250 nL/min and 20 °C. A 55 min-long
230 gradient was employed with H₂O and ACN as mobile phases A and B, respectively, both with 0.1%

231 formic acid. The following linear gradient was used: 1% B for 5 min; 1–5% B in 2 min; 5–35% B in
232 38 min; 35–50% B in 5 min; 50–90% B in 5 min. Finally, the column was washed at 90% B for 10
233 min and then equilibrated at 1% B for 20 min.

234 Peptide spectra were acquired in the 380–1800 m/z range at 30,000 resolution (full width at half
235 maximum, FWHM, at m/z 400) for the full scan. MS/MS spectra were acquired at 15,000 resolution
236 (FWHM, at m/z 400) in top 10 data-dependent acquisition (DDA) mode with the rejection of singly
237 charged ions and unassigned charge states. Precursors were fragmented by higher-energy collisional
238 dissociation (HCD) with 35% normalized collision energy and 2 m/z isolation window (other
239 fragmentation techniques, such as infrared multiphoton dissociation, could provide additional
240 information due to the formation of more secondary fragments and reduced ion losses (Bianco et al.,
241 2014). Dynamic exclusion was enabled with a repeat count of 1 and a repeat duration of 30 s with an
242 exclusion duration of 20 s. For each sample, three technical replicates were performed. Raw data files
243 were acquired by Xcalibur software (version 2.2, Thermo Fisher Scientific).

244 **2.5 Analysis of short-chain peptide mixture by ultra-high performance liquid chromatography-** 245 **MS/MS**

246 Short-chain peptide mixture obtained from SEC and UFM were analyzed by LC-HRMS in a suspect
247 screening fashion as previously described (Cerrato, Aita, et al., 2020) using a Vanquish binary pump
248 coupled to a hybrid quadrupole-Orbitrap Q Exactive mass spectrometer (Thermo Fisher Scientific)
249 through a heated electrospray source. Samples were separated by a Kinetex XB-C18 (100 × 2.1 mm,
250 particle size 2.6 µm, Phenomenex, Torrance, CA, USA) operated at 40 °C. Spectra were acquired in
251 the positive ion mode range m/z 150-750 with a resolution (full width at half maximum, FWHM, m/z
252 200) of 70,000. For each sample, two individual runs were acquired for natural and modified short
253 peptides using two dedicated inclusion lists containing the exact m/z of the protonated ions of all
254 unique short peptide masses. The inclusion lists were prepared using MatLab R2018, as previously
255 described (Cerrato, Aita, et al., 2020). The acquisition of the higher collisional dissociation (HCD)
256 MS/MS spectra was performed using the top 5 data-dependent acquisition (DDA) mode at 35%

257 normalized collision energy and 35,000 (FWHM, m/z 200) resolution. All samples were run in
258 triplicate.

259 The identification of the short endogenous peptidome was achieved thanks to a dedicated data
260 processing workflow implemented on Compound Discoverer 3.1 (Thermo Fisher Scientific) by our
261 research group (Cerrato, Aita, et al., 2020). The strategy allowed to extract the m/z from the RAW
262 data files, align the runs, and remove blank signals and masses not associated with at least one MS/MS
263 spectrum. Moreover, the workflow allowed to filter out all masses not present in the mass list (the
264 same employed for short peptide data acquisition). The identification of the short sequences was
265 achieved after manual interpretation of the MS/MS spectra aided by the match of the in silico spectra
266 generated by mMass (Strohalm et al., 2010).

267 **2.6 Cell culture conditions**

268 Human hepatic HepG2 cells were bought from ATCC (HB-8065, ATCC from LGC Standards, Milan,
269 Italy) and intestinal Caco-2 cells were obtained from INSERM (Paris, France). Both cell lines were
270 cultured in DMEM high glucose with stable L-glutamine, supplemented with 10% FBS, 100 U/mL
271 penicillin, 100 µg/mL streptomycin (complete growth medium) with incubation at 37 °C under 5%
272 CO₂ atmosphere..

273 **2.7 MTT assay**

274 A total of 3 x 10⁴ HepG2 and Caco-2 cells/well were seeded in 96-well plates and treated with 0.1,
275 0.5, 1.0, and 2.0 mg/mL of S, M, and T peptide mixtures, or vehicle (H₂O) in complete growth media
276 for 48 h at 37 °C under 5% CO₂ atmosphere. Subsequently, the treatment solvent was aspirated and
277 100 µL/well of 3-(4,5-dimethylthiazol-2-yl)-2,5-diphenyltetrazolium bromide (MTT) filtered
278 solution added. After 2 h of incubation at 37 °C under 5% CO₂ atmosphere, 0.5 mg/mL solution was
279 aspirated and 100 µL/well of the lysis buffer (8 mM HCl + 0.5% NP-40 in DMSO) added. After 5
280 min of slow shaking, the absorbance at 575 nm was read on the Synergy H1 fluorescence plate reader
281 (Biotek, Bad Friedrichshall, Germany).

282 **2.8 HMGC_oAR activity assay**

283 The assay buffer, NADPH, substrate solution, and HMGCoAR were provided in the HMGCoAR
284 Assay Kit (Sigma). The experiments were carried out following the manufacturer's instructions at
285 37 °C. In particular, each reaction (200 µL) was prepared adding the reagents in the following order:
286 1 X assay buffer, S and M peptides mixtures (at final concentrations of 0.1, 0.12, 0.15, 0.175, 0.2, 0.3
287 mg/mL, and the total hydrolysate T (at final concentrations of 0.2, 0.25, 0.3, 0.4, 0.5 mg/mL) or
288 vehicle (C), the NADPH (4 µL), the substrate solution (12 µL), and finally the HMGCoAR (catalytic
289 domain) (2 µL). Subsequently, the samples were mixed and the absorbance at 340 nm read by a
290 microplate reader Synergy H1 from Biotek at time 0 and 10 min. The HMGCoAR-dependent
291 oxidation of NADPH and the inhibition properties of lupin peptides were measured by absorbance
292 reduction, which is directly proportional to enzyme activity.

293

294 **2.9 Western blot analysis**

295 A total of 1.5×10^5 HepG2 cells/well (24-well plate) were treated with S at a concentration of 0.5
296 mg/mL and with M and T at a concentration of 1 mg/mL, or with the reference compound MonK at
297 1 µM, or vehicle (H₂O), for 24 h. After each treatment, cells were scraped in 30 µL ice-cold lysis
298 buffer [RIPA buffer + inhibitor cocktail + 1:100 PMSF + 1:100 Na-orthovanadate] and transferred in
299 an ice-cold microcentrifuge tube. After centrifugation at 13300g for 15 min at 4 °C, the supernatant
300 was recovered and transferred into a new ice-cold tube. Total proteins were quantified by Bradford
301 method and 50 µg of total proteins loaded on a pre-cast 7.5% Sodium Dodecyl Sulphate -
302 Polyacrylamide (SDS-PAGE) gel at 130 V for 45 min. Subsequently, the gel was pre-equilibrated
303 with 0.04% SDS in H₂O for 15 min at room temperature (RT) and transferred to a nitrocellulose
304 membrane (Mini nitrocellulose Transfer Packs,) using a trans-Blot Turbo at 1.3 A, 25 V for 7 min.
305 Target proteins, on milk or BSA blocked membrane, were detected by primary antibodies as follows:
306 anti-SREBP2, anti-LDLR, anti-HMGCoAR, anti-PCSK9, anti-HNF1- α and anti- β -actin. Secondary
307 antibodies conjugated with HRP and a chemiluminescent reagent were used to visualise target
308 proteins and their signal was quantified using the Image Lab Software (Biorad). The internal control

309 β -actin was used to normalize loading variations. The anti-PCSK9 and anti-HNF1- α primary
310 antibodies were used after the complete removal of primary and secondary antibodies from
311 membranes were the SREBP-2 and the HMGCoAR proteins, respectively, were previously detected,
312 since the molecular weights of these proteins are similar.

313 **2.10 Assay for evaluation of fluorescent LDL uptake by HepG2 cells**

314 A total of 3×10^4 HepG2 cells/well were seeded in 96-well plates and kept in complete growth medium
315 for 2 days before treatment. On the third day, cells were treated with S peptides mixture at a
316 concentration of 0.5 mg/mL and with M and T peptides mixtures at a concentration of 1 mg/mL, or
317 with the reference compound Monacolin K (MonK) at 1 μ M or vehicle (H_2O) for 24 h. At the end of
318 the treatment period, the culture medium was replaced with 50.0 μ L/well LDL-DyLight™ 550
319 working solution. The cells were additionally incubated for 2 h at 37 °C and then the culture medium
320 was aspirated and replaced with PBS (100 μ L/well). The degree of LDL uptake was measured using
321 the Synergy H1 fluorescent plate reader from Biotek (excitation and emission wavelengths 540 and
322 570 nm, respectively).

323 **2.11 *In vitro* DPPIV activity assay**

324 The *in vitro* experiments were carried out in duplicate in a half-volume 96-well solid plate (white).
325 Each reaction (50 μ L) was prepared adding the reagents in a microcentrifuge tube in the following
326 order: 1 X assay buffer [20 mM Tris-HCl, pH 8.0, containing 100 mM NaCl, and 1 mM EDTA] (30
327 μ L), S, M and T peptides mixtures at final concentrations of 0.1, 0.5, 1.0, 1.5 and 2.0 mg/mL or
328 vehicle (10 μ L) and finally the DPPIV enzyme (10 μ L). Afterward, the samples were mixed and the
329 50 μ L were transferred in each plate well. Each reaction was started by adding 50 μ L of substrate
330 solution (200 μ M H-Gly-Pro-7-amido-4-methylcoumarin (AMC)) to each well and incubated at 37
331 °C for 30 min. Fluorescence signals were measured using the Synergy H1 fluorescent plate reader
332 from Biotek (excitation and emission wavelengths 360 and 465 nm, respectively). The DPPIV
333 enzyme and the substrate solution were provided by Cayman Chemicals (Michigan, USA).

334 **2.12 Evaluation of the inhibitory effect of hempseeds peptides on cellular DPP-IV activity**

335 A total of 5×10^4 Caco-2 cells/well were seeded in black 96-well plates with clear bottoms. On the
336 second day after seeding, spent media was discarded and the cells were treated with 1.0 and 2.0
337 mg/mL of S, M, and T peptides mixtures, or Sitagliptin (100 nM) as reference compound, or vehicle
338 (H_2O) in growth medium for 3h at 37 °C. Subsequently treatments were removed and 40 μ L of Gly-
339 Pro-AMC substrate were added to each well at the concentration of 25 μ M in PBS. Fluorescence signal
340 (excitation and emission wavelengths 350 and 450 nm, respectively) was recorded after 30 min using
341 a Synergy H1 microplate reader.

342

343 **2.13 *Ex vivo* DPP-IV Activity Assay**

344 Human serum sterile filtered commercially available from Sigma-Aldrich (Cat. N° H4522-100 mL)
345 were aliquoted 40 μ L/well in black 96-well plates and 10 μ L of S and M peptides mixtures (at final
346 concentrations of 1.0 and 2.0 mg/mL) and Sitagliptin (at a final concentration of 100 nM) were added
347 and the plate was incubated for 1h at 37 °C. Subsequently, 50 μ L of Gly-Pro-AMC was added to each
348 well to achieve a final substrate concentration of 25.0 μ M. Fluorescence signals (ex./em. 350/450
349 nm) were then recorded using a Synergy H1 microplate reader.

350

351 **2.14 *In vitro* measurement of the ACE inhibitory activity**

352 ACE inhibitory activity was tested by measuring with HPLC the formation of hippuric acid from
353 hippuryl-histidyl-leucine, used as a mimic substrate for ACE I. Test was performed in 100 mM Tris-
354 HCOOH, 300 mM NaCl pH 8.3 buffer, and using ACE from porcine kidney (Sigma-Aldrich, Milan,
355 Italy). S, M and T peptides mixtures were tested at 1.0 mg/mL and IC₅₀ value is the concentration
356 needed to observe a 50% inhibition of ACE activity. All experimental details of samples preparation
357 and analyses conditions have been published elsewhere (Boschin et al., 2014a) (Boschin et al.,
358 2014b).

359

360 **2.15 Statistical analysis**

361 Three independent T hydrolysates from which three independent M and S fractions were produced.
362 Each independent sample was analytical characterized, and the sequences of the identified peptides
363 are the same among the three independent T, M, and S samples, respectively. For the biological
364 characterization, a pool of the three independent hydrolysates was produced and tested performing
365 all the biological experiments. Statistical analyses were carried out by One-way analysis of variance
366 (ANOVA, Graphpad Prism 9) followed by Dunnett's test. Values were expressed as means \pm s.d.; P-
367 values <0.05 were considered to be significant.

368

369 **3. Result and Discussion**

370 **3.1 Hempseed peptides production and peptidomics analysis**

371 Hemp seeds contain 20–25% protein, rich in essential amino acids for maintaining good health
372 (Farinon et al., 2020). Hemp seed proteins possess high bioavailability and digestibility, contain
373 hypoallergenic peptides whose absorption is improved by the fiber complex, and have a subtle
374 aromatic profile, a balanced food source for human nutrition (Nwachukwu & Aluko, 2021). The
375 current trend is to relaunch this underexploited plant to obtain protein seeds with benefits for various
376 diseases that have been medically proven (Hertzler et al., 2020). Recent investigations have
377 demonstrated that peptides produced by enzymatic hydrolysis of hempseed proteins provide several
378 biological activities, including antihypertensive activity (Malomo et al., 2015), anti-inflammatory
379 activity (Cruz-Chamorro et al., 2022), hypocholesterolemic activity (Zanoni et al., 2017), antioxidant
380 activity (Pontonio et al., 2020), inhibitory activity on HMGCoAR (Aiello et al., 2017), and anti-
381 diabetic properties (Lammi, Bollati, et al., 2019). Most of these works focus on a limited number of
382 medium-sized peptides, namely those with more than seven amino acids in their sequences.

383 In contrast, only one report has obtained an UFM extract in which the molecular weight distribution
384 of hemp peptides estimated by MALDI-TOF/TOF mainly comprises 2–3 amino acid residues (Wei
385 et al., 2021). It has been reported that short oligopeptides, especially dipeptides or tripeptides, are the
386 best candidate since they can easily be absorbed, resisting to hydrolysis by gastrointestinal proteases
387 and serum peptidases, and can be transported in their bioactive forms to target tissues (Wang et al.,
388 2019). Short peptide sequences have been largely neglected to date, compared to medium- and long-
389 chain peptides, which have long been investigated by borrowing the analytical technologies from
390 bottom-up proteomics (Fricker, 2015). Short peptides show a more remarkable resemblance to polar
391 metabolites than longer peptides for their low molecular weights and wide range of physicochemical
392 properties (acid-base properties and polarity). An analytical platform was set up in our laboratory
393 based on a purification step dedicated explicitly to the separation of short-chain peptide mixture,
394 suspect screening data acquisition, and a customized data processing workflow on Compound

395 Discoverer software in a metabolomics-based fashion to deal with the untargeted identification of
396 short peptide sequences (Cerrato, Aita, et al., 2020).

397 In our previous works, a solid phase purification based on graphitized carbon black (GCB) material
398 was employed to enrich short peptides (Piovesana et al., 2019). For nutraceutical applications, which
399 have the final purpose of introducing a potential new product with multifunctional activity on the
400 market, the industrial scale-up of purification and separation processes is essential to treat a high
401 amount of samples. Using material as GCB poses several limitations for routinary purification
402 because the analytical process is laborious and time-consuming. For basic peptides, for instance, a
403 backflushing elution is needed. Moreover, the GCB is produced at high temperatures, and some
404 reproducibility problems could occur between two different preparation batches or manufacturers.
405 For these reasons, the remarkable production volumes of peptide mixtures for nutraceutical purposes
406 have generated a strong interest in alternative purification procedures, mainly due to their relevant
407 impact on manufacturing costs. Because of its flexibility, preparative liquid chromatography is
408 nowadays the method of choice in these applications, allowing one to choose case-by-case the
409 experimental conditions that most suitably fit that particular purification problem (De Luca et al.,
410 2021). In line with literature evidences (Malomo et al., 2015), the DH (%) of Alcalase derived total
411 hydrolysate (T) was $27.8 \pm 2.2\%$, and the peptide concentration, which was determined by GoA assay
412 (Lammi et al., 2016), is $308,03 \pm 10,5 \mu\text{g}/\mu\text{L}$. Two analytical techniques were chosen and compared
413 in this work: SEC and UFM. The use of SEC permitted obtaining two distinct fractions, as shown in
414 Figure 1S, containing medium-chain (1-5 min) and short-chain peptides (5-10 min). In contrast, using
415 UFM led to obtaining a single fraction consisting of only short-chain peptide mixture.

416 The obtained fractions were analysed differently; those containing short-chain peptide mixture was
417 submitted to a suspect screening approach on UHPLC-HRMS instrumentation, while a typical
418 proteomics experiment by nanoLC-HRMS was employed to analyse the fraction containing medium-
419 chain peptide mixture.

420 The suspect screening approach was based on using inclusion lists in the mass spectrometric method
421 that bypasses the limitations of data-dependent acquisition mode when comprehensive lists of the
422 analytes are available (Cerrato, Aita, et al., 2020). Moreover, the data processing workflow allowed
423 extracting the m/z from the raw data files, aligning the features in the different samples, removing
424 compounds present in the blank sample, predicting the molecular formulas from the accurate masses
425 and isotopic patterns, and associating the predicted formula to those of the short peptide sequences
426 listed in the short peptide databases that were also employed for data acquisition. After careful manual
427 validation of the putative peptides based on the peculiar short peptide fragmentation pathways, 559
428 short peptides and 557 peptides were tentatively isolated in hemp seed by SEC and UFM,
429 respectively. Table S1 reports, for short-chain peptides isolated by SEC and UFM, respectively,
430 detailed data on the tentatively identified sequences, including retention time, proposed formula,
431 experimental m/z, MS accuracy, and primary diagnostic product ions. Since Leu and Ile cannot be
432 distinguished by MS/MS (MS3 experiments are needed) (Cerrato, Aita, et al., 2020), the
433 nomenclature Xle was employed throughout the manuscript and Supplementary Materials for
434 indicating either Leu or Ile in a peptide sequence. Five hundred forty-eight peptides (98%) were
435 common in the two isolation procedures establishing no significant differences between the
436 techniques employed. Of the 568 annotated short peptides, 224 (39.3%) were dipeptides, 176 (31%)
437 were tripeptides, and 168 (29.7%) were tetrapeptides with a molecular weight in the range 174.1-
438 587.3 Da.

439 Due to its simplicity, UFM represents the most suitable technique for routine analysis and industrial
440 scale-up. Still, at this stage, SEC had the advantage of purifying and recovering both short-chain and
441 medium-sized peptides for comparing the biological activity of the two distinct fractions and selecting
442 those more likely to be used to prepare nutraceuticals.

443 The identification of medium-chain peptides was achieved by using an established peptidomics
444 approach. Currently, techniques borrowed from shotgun proteomics are the most efficient methods
445 for identifying peptides in complex samples, such as food protein digests or native peptide extracts.

446 By this approach, 278 medium-chain peptides were identified; data are reported in Supplementary
447 Material Table S2.

448

449 **3.2 Multifunctional health-promoting effects of hemp seed peptides**

450 **3.2.1 Activity of hempseed peptides on cholesterol metabolism pathway**

451 **3.2.1.1. Hempseed peptides inhibit the *in vitro* HMGCoAR activity**

452 *In vitro* experiments were carried out using the purified catalytic domain of the enzyme HMGCoAR,
453 a known target of statins. The results suggested that the total hydrolyzate (T), the short- (S), and
454 medium- (M) chain peptide mixtures can inhibit the enzyme activity in a dose-dependent manner
455 with IC₅₀ values equal to 0.38 ± 0.012 , 0.18 ± 0.005 , and 0.25 ± 0.009 mg/mL, respectively (Figure
456 1A-B). Improved inhibitory activity of S fraction appears evident since it is 2-fold more active than
457 the total hydrolyzate. Comparison with the literature shows that the peptides obtained by hydrolyzing
458 hempseed proteins with Alcalase are more active than those obtained by hydrolyzing these proteins
459 with pepsin (IC₅₀ 0.8 mg / mL) (Zanoni et al., 2017), trypsin (IC₅₀ 0.65 mg/mL)(Aiello et al., 2017),
460 whereas the peptides obtained using pancreatin are inactive as inhibitors of HMGCoAR (Aiello et al.,
461 2017). The peptides obtained by co-digesting hemp seed proteins with pepsin, trypsin, and pancreatin
462 can inhibit the HMGCoAR enzyme but not in a dose-dependent manner (Aiello et al., 2017).

463

464 **3.2.1.2 Hempseed peptides modulate the cholesterol metabolism pathway**

465 Based on the ability of S, M, and T peptides mixtures to inhibit the HMGCoAR enzyme, in-depth
466 experiments (Figure 2S A-C) were performed to establish the mechanism of action through which
467 they exert a cholesterol-lowering effect in human hepatic HepG2 cells.

468 Initially, MTT experiments were carried out to evaluate the effect of the S, M, and T peptides on
469 hepatic cell viability. Results indicated that in the concentration range 0.1 - 2.0 mg/mL, any samples
470 showed cell viability-reducing effects (Figure 1S A-C). Then, the HepG2 cells were treated with S
471 peptides at the concentration of 0.5 mg/mL¹ and with M and T peptides at the concentration of 1

472 mg/mL. MonK (1 μ M) was used as the reference compound, being responsible for the cholesterol-
473 lowering activity in all nutraceuticals based on RYR extract. All tested peptides (S, M, and T)
474 modulate cholesterol metabolism by activating the LDLR and confirming that S peptides are 2- fold
475 more active than M and T (Figure 2). More in detail, S, M, and T induced an increase of mature
476 SREBP-2 transcription factor (65 KDa isoform) of $34.7 \pm 4.5\%$, $43.5 \pm 17.2\%$, and $43.5 \pm 16.5\%$,
477 respectively (Figure 2A). The increase of this transcription factor determined an increase in LDL
478 receptor levels by $55.2 \pm 4.7\%$, $85.1 \pm 21.4\%$, and $80.2 \pm 20.3\%$ for S, M, and T, respectively (Figure
479 2B). In agreement with these results, an increase in HMGCoAR protein levels of $30.2 \pm 10.8\%$, 32.8
480 $\pm 10.6\%$, and $56.2 \pm 7.2\%$ was observed upon HepG2 treatments with S, M, and T peptides,
481 respectively (Figure 2C). Results suggested that hemp seed peptides modulate cholesterol metabolism
482 with a mechanism of action that is similar to MonK. Notably, MonK increases mature SREBP-2
483 protein levels by $41.3 \pm 14.0\%$, LDLR by $48.0 \pm 6.5\%$ and HMGCoAR by $33.4 \pm 21.5\%$ (Figure 2
484 A-C).

485 From a functional point of view, S, M, and T increase the ability of HepG2 cells to absorb LDL from
486 the extracellular environment with a final cholesterol-lowering effect. Also, in this case, S peptides
487 are 2-folds more active than M and T (Figure 2D). In particular, the S increased the ability of cells to
488 clear extracellular LDL by $183.8 \pm 13.7\%$ at 0.5 mg/mL, whereas both M and T up to $147.7 \pm 1.9\%$
489 and $211.4 \pm 21.3\%$ at 1.0 mg/mL, respectively (Figure 2D). In parallel, MonK increased the functional
490 capacity of cells to uptake LDL by $126.9 \pm 11.0 \pm 12.6\%$, $39.3 \pm 15.8\%$, and $42.7 \pm 9.1\%$, respectively
491 (Figure 2D). Indeed, Figure 2D clearly shows that the functional capacity of HepG2 cells to absorb
492 extracellular LDL after treatment with M and T peptides and, in particular, S peptides, at half of the
493 concentration of M and T, is precisely equal to the HepG2 cell capacity to absorb extracellular LDL
494 after treatment with MonK at the concentration of 1 μ M.

495 In addition, the PCSK9 protein levels decrease by $38.1 \pm 12.6 \%$, $38.2 \pm 15.8 \%$, and $42.6 \pm 9.1\%$,
496 after treatment with S, M and T peptides, respectively (Figure 2E). These reductions are due to the
497 ability of these samples to decrease the levels of HNF-1alpha transcription factor by $24.1 \pm 8.4\%$,

498 17.2 ± 17.7%, and 8.6 ± 10.9%, respectively (Figure 2F). In parallel, the experiments were carried
499 out using MonK, confirming its ability to increase PCSK9 levels by 25.8 ± 2.4% and HNF-1alpha by
500 27.1% ± 5.7, with a negative effect on active LDLR levels localized on the surface of the hepatocytes.
501 These results, therefore, highlight a new and different cholesterol-lowering mechanism from that
502 exerted by MonK. The behavior of these peptides also differs significantly from what is known in the
503 literature. The peptic hydrolyzate cannot modulate any effect on the PCSK9 pathway (Aiello et al.,
504 2017).

505 **3.2.2 Assessment of the DPP-IV inhibitory activity of hempseed peptides.**

506 *In vitro* experiments were carried out using the recombinant form of the enzyme DPP-IV, a known
507 target for treating type 2 diabetes. The results showed that the S, M, and T peptides inhibit the DPP-
508 IV activity with IC₅₀ values of 0.82 ± 0.12, 1.17 ± 0.09, and 1.36 ± 0.08 mg/mL, respectively (Figure
509 3A). These results suggest that the S peptides are about 2 times more active than the total hydrolyzate.
510 Recent shreds of evidence indicated that tryptic and peptic hydrolysates (1.0 mg/mL) inhibit the
511 enzyme activity by 17.5 and 32.0%, respectively (Lammi, Bollati, et al., 2019), clearly suggesting
512 that the S, M, and T peptides are more active.

513 Based on these results, *in situ* experiments were carried out to evaluate the ability of hempseed
514 peptides to inhibit the DPP-IV enzyme expressed on the membrane of human intestinal Caco-2 cells.
515 Initially, MTT experiments were conducted to evaluate the potential cytotoxic effects of the samples
516 on intestinal Caco-2 cells. The results showed no effects of reduction of cell viability were highlighted
517 in the range of concentrations tested (Figure 2S (C-D-E)).

518 Then, Caco-2 cells were treated with S, M, and T peptides (1 and 2 mg / mL). The results showed
519 that S, M, and T inhibit the DPP-IV enzyme expressed on the membranes of Caco-2 cells by 20.2 ±
520 6.3%, 15.4 ± 11.9%, and 19.7 ± 10.6%, respectively, at 1 mg / mL and by 47.6 ± 4.2%, 31.3 ± 6.3%
521 and 35.4 ± 2.7% respectively. at 2 mg/mL (Figure 3B). In parallel, sitagliptin at 100 nM inhibits the
522 enzyme by 46.8 ± 0.6% (Figure 3B).

523 Finally, the S and M peptides were tested *ex vivo* to evaluate their ability to inhibit the circulating
524 form of the DPP-IV enzyme present in human serum. Indeed, the results demonstrate that S and M
525 reduce the activity of the circulating form of DPP-IV by $47.1 \pm 2.4\%$ and $36.5 \pm 4.7\%$, at 1 mg/mL,
526 respectively, and by $52.9 \pm 1.6\%$ and $38.1 \pm 3.1\%$, at 2 mg / mL, respectively (Figure 3C).

527

528 **3.2.3 Anti-ACE and antioxidant activity of the hempseed peptide fractions**

529 *In vitro* experiments were carried out using the porcine kidney ACE enzyme, a known target for the
530 treatment of hypertension. The results showed that at the fixed concentration of 1 mg/mL, the S, M,
531 and T peptides inhibited the ACE enzyme by $57.5 \pm 0.1\%$, $15.7 \pm 0.3\%$, and $32.4 \pm 0.5\%$, respectively,
532 towards control ($p < 0.0001$) (Figure 4). From the statistical analysis, it appears clear that the S
533 peptides are about three times more active than the M peptides ($p < 0.0001$) and that they clearly
534 represent the active component of the total hydrolyzate T ($p < 0.0001$) (Figure 4). Notably, since in
535 the T sample, M and S peptides are concomitantly available, the enzyme may recognize and bind
536 both short-chain and medium-chain peptides which can bind the ACE enzyme exerting the inhibitory
537 effect with an additive/synergistic behavior. These results suggested that the ACE inhibitory activities
538 exhibited by our samples are lower than hempseed peptide mixture obtained using Alcalase by Girgih
539 and co-workers (Girgih et al., 2014).

540 Two different assays were used to evaluate the antioxidant activity: the first was the 2,2-Diphenyl-1-
541 picrylhydrazyl (DPPH) assay, with which the ability of the samples to eliminate the DPPH radical
542 and, therefore, the scavenging ability of free radicals is assessed; the second assay was FRAP (Ferric
543 Reducing Antioxidant Power), which measures the ability of antioxidants to reduce the Fe^{3+} complex
544 to the reduced Fe^{2+} complex.

545 Figure 5 shows the *in vitro* effects of the direct antioxidant activity of S, M, and T peptides by DPPH
546 assay. The results clearly suggest that the samples express antioxidant power with a dose-response
547 trend (Figure 5A). In particular, at concentrations of 0.5, 1.0, 2.5 and 5.0 mg / ml, the S peptides have
548 scavenger activity equal to $10.9 \pm 2.4\%$, $18.3 \pm 2.9\%$, $26.8 \pm 4.8\%$ and $42.3 \pm 4.6\%$; the M peptides

549 equal to $8.9 \pm 0.5\%$, $12.7 \pm 4.6\%$, $18.8 \pm 2.6\%$ and $25.8 \pm 7.3\%$; while the T peptides have DPPH
550 radical removal activities equal to $27.3 \pm 1.6\%$, $32.1 \pm 1.2\%$, $39.3 \pm 1.5\%$ and $44.9 \pm 0.9\%$,
551 respectively. Our results suggest that T peptides are more effective to scavenge the DPPH radicals
552 than S and M samples, respectively. This difference may be explained considering that in T sample
553 both short- and medium chains peptides are concomitantly present exerting the antioxidant activity
554 with a synergistic effects among peptides.

555 Figure 5B shows the *in vitro* effects of the FRAP assay's direct antioxidant activity of the S, M, and
556 T peptides. The results clearly indicate that the peptides express a reducing capacity in a dose-
557 response manner (Figure 5B). In particular, at concentrations of 0.1, 0.5, 1.0 and 2.5 mg / ml, S
558 peptides increase iron reduction by $528.9 \pm 53.8\%$, $1936 \pm 234.8\%$, $3284 \pm 390.8\%$, $5238 \pm 523.5\%$,
559 M peptides by $44.44 \pm 9.6\%$, $197,2 \pm 29.3\%$, $377.8 \pm 81.8\%$ and $838.9 \pm 194.1\%$, finally the T
560 peptides increase the reduction of iron by $888.7 \pm 62.7\%$, $1678 \pm 133.8\%$, $2546 \pm 181.0\%$ and 4654
561 $\pm 405.5\%$, respectively. Our results suggest that T peptides exert a FRAP activity with a trend which
562 is equal to S clearly underlining that short-chain peptide mixture is the active components of the T
563 samples. This explanation is reforced by the fact that M peptide mixture is less active than M peptides
564 in FRAP activity.

565 Many physicochemical factors may influence the ability of peptides to exert antioxidant activity.
566 Although certain aspects of the structure-function relationship of antioxidant peptides are still poorly
567 understood, chain length, type, composition, sequence, and the location of specific amino acids in a
568 peptide chain have been suggested to be critical issues for exerting the antioxidant property (Gallego,
569 Mora, & Toldrá, 2018). In this context, short peptides may often be potent antioxidants. Literature
570 indicates that, besides containing hydrophobic amino acids, such as Leu or Val, in their N-terminal
571 regions, peptides containing nucleophilic sulfur-containing amino acid residues (Cys and Met),
572 aromatic amino acid residues (Phe, Trp, and Tyr) and/or the imidazole ring-containing His are
573 generally found to possess strong antioxidant properties (Santos-Sánchez et al., 2022).

574 Our results are in agreement with other studies demonstrating that hempseed peptides generated by
575 alcalase, alcalase + flavourzyme, and pepsin + pancreatin, exert radical scavenging activity and
576 increase the total antioxidant status (Santos-Sánchez et al., 2022). On the contrary, hempseed peptides
577 produced by neutrase, and proteases preparation [AFP 4000 (AFP), HT Proteolytic Concentrate (HT),
578 Protease G (Pro-G), actinidin, protamex, and zingibain] only show radical scavenging activity
579 (Santos-Sánchez et al., 2022).

580

581 **3.3 Assessment of the intestinal trans-epithelial transport of hempseed peptides.**

582 In the field of food bioactive peptides, one of the main limitations, which affects their fast exploitation
583 on the market as nutraceuticals and/or functional foods, is represented by their low metabolic stability
584 and bioavailability at the intestinal level (Amigo & Hernández-Ledesma, 2020). Short-chain peptide
585 are more easily transported to the bloodstream and the presence of bioactive peptides in the blood,
586 after ingestion of protein hydrolysates derived from both vegetal and animal food source, have been
587 detected (Ejima et al., 2018; Iwai et al., 2005; Segura-Campos et al., 2011). Indeed, intestinal cells
588 are the first physiological barrier encountered by food peptides and/or hydrolysates. In general, when
589 the protein hydrolysates and/or peptides come in contact with human enterocytes, two main
590 phenomena may occur: peptides are in part transported by the cells and in part metabolized by the
591 same cellular environment, even though the metabolic degradation of bioactive peptides does not
592 always mean that the mixtures lose the bioactivity (Bollati et al., 2022; Lammi et al., 2021). Hence,
593 the intestine is a very complex physiological environment that actively modulates the bioactivity of
594 protein hydrolysates and/or peptides through direct effects on their chemical compositions and
595 peptidomics profiles. Therefore, it is crucial to realize *in vitro* experiments for mimicking the
596 intestinal transport of food protein hydrolysates before performing expensive *in vivo* experiments to
597 confirm their health-promoting activity. Worldwide, differentiated human intestinal Caco-2 cells are
598 successfully employed as a reliable model for *in vitro* evaluation of food bioactive peptide propensity
599 to be transported by intestinal cells. Taking this into account, Caco-2 cells have been differentiated

600 and incubated on their apical (AP) side with S at the concentration of 1 mg/mL for 2 h. Then, AP and
601 basolateral (BL) solutions were collected and analyzed by UHPLC-HRMS. Focusing on dipeptides,
602 tripeptides, and tetrapeptides results clearly indicated that out of the 569 hempseed peptides which
603 were identified in the starting S fraction of the hempseed hydrolysate, only 279 peptides had been
604 identified in the BL solution, clearly indicating that only 49% of the short peptides are transported
605 intact by differentiated intestinal cells. In general, food-derived peptides may be transported across
606 the intestinal brush-border membrane into the bloodstream *via* one or more of the following routes:
607 (i) peptide transport 1 (PepT1)-mediated route, (ii) paracellular route via tight junctions (TJs), (iii)
608 transcytosis route, and (iv) passive transcellular diffusion (Lammi et al., 2021).

609 Certainly, peptide size, charge, hydrophobicity, and degradation due to the action of peptidases are
610 among the main factors influencing the absorption through one or more of these routes. In general,
611 short peptides, such as dipeptides and tripeptides, are preferentially transported by PepT1, due to its
612 high capacity, low affinity, and high expression in the intestinal epithelium (Lammi et al., 2020),
613 whereas highly hydrophobic peptides are transported by simple passive transcellular diffusion or by
614 transcytosis (Lammi et al., 2020).

615 Using the BIOPEP-UWM database (<https://biochemia.uwm.edu.pl/biopep-uwm/>), most of the S
616 peptides transported by intestinal cells display DPP-IV and ACE inhibitory properties as well as
617 antioxidant activity.

618 Mature enterocytes develop microvilli that function as the gastrointestinal tract's primary surface of
619 nutrient absorption. Their membrane is packed with enzymes that favor the breakdown of complex
620 nutrients into simpler compounds that are more easily absorbed. The dynamic equilibrium between
621 bioactive peptide degradation and transport is crucial from a physiological point of view. Possessing
622 a wide range of membrane peptidases naturally expressed by the AP side of enterocytes, including
623 DPP-IV and ACE (Lammi et al., 2021), a differentiated Caco-2 model is also a reliable tool for
624 investigating the proteolytic activity of the brush border barrier. Under this hypothesis, our results
625 indicate that out of the total 569 short peptides identified in the S fraction of total hydrolysate, 471

626 are present in the AP solution, suggesting that about 17.2% (15 dipeptides, 35 tripeptides, and 36
627 tetrapeptides) of peptides which were present in the original short peptide fraction are metabolized
628 by intestinal cells, or they are uptaken and intracellular used by Caco-2 cells during the 2 hr of
629 incubation with the cells. Interestingly, short peptides containing in their N-terminal methionine (M)
630 and tryptophan (W) residues are not able to be transported by intestinal cells; this particular aspect
631 may be explained considering that the brush border membranes express aminopeptidase N and
632 ectopeptidase and from its position which faces with intestinal lumen it can recognize peptides
633 containing in the N-terminal, M, and W metabolizing them (Röhnert et al., 2012).

634

635 **4. Conclusions**

636 Using a multidisciplinary approach, this bottom-up study clearly supports the pleiotropic activity
637 exerted by hempseed short-chain peptide mixture. Indeed, hempseed peptide mixture enriched with
638 short-chain ones is endowed with potential hypocholesterolemic, anti-diabetic, hypotensive, and
639 antioxidant activities, respectively. In this study, we have produced, analyzed, and detailed
640 characterized hempseed hydrolysate providing a comprehensive picture of its multifunctional power.
641 Of course, the bio-activity of short-chain peptide mixture reflects the composition of the fraction in
642 which being present hundreds of peptides some synergistic interaction may occur, clearly suggesting
643 that not only the size of the peptides contributes to the biological activity but rather than the force of
644 the synergistic/additive interaction among the species within the fraction may play a key role in the
645 multifunctional effect. This preclinical assessment demonstrates that our hempseed peptide mixture,
646 which is easily scaling up at the industrial level, may be potentially exploited as new valuable
647 ingredients for the development of innovative functional foods and or dietary supplements useful for
648 the prevention of metabolic syndrome. Of course, to achieve this important goal, further experiments
649 have to be performed to confirm the multifunctional properties of these hempseed peptides using
650 animal models.

651

652 **Fundings**

653 This research was in part funded by Sapienza University of Rome – Progetto per Avvio alla Ricerca
654 – Tipo 2 – “Development of innovative strategies for the untargeted identification of natural and
655 modi-fied short-sized bioactive peptides”, grant number AR22117A815792CD

656

657 **Acknowledgements**

658 The authors gratefully acknowledge Carlo Sirtori Foundation (Milan, Italy) for having provided part
659 of the equipment used in this experimentation. In addition, The authors gratefully acknowledge the
660 financial support from the China Scholarship Council for a fellowship to J.L.

661

662 **Patent:**

663 Italian Patent provisional number 102022000003347 " Metodo per la caratterizzazione di peptidi corti
664 da canapa industriale" Inventors Anna Arnoldi, Chiara Cavaliere, Anna Laura Capriotti, Andrea
665 Cerrato, Aldo Laganà, Carmen Lammi, Carmela Maria Montone, Susy Piovesana – property:
666 Università degli Studi di Milano e Università di Roma La Sapienza.

667

668 *CRedit authorship contribution statement*

669 **Andrea Cerrato:** Investigation, Methodology, Data Curation. **Carmen Lammi:** Conceptualization,
670 Supervision, Formal analysis, Writing - Original Draft, Writing - Review & Editing. **Anna Laura**
671 **Capriotti:** Conceptualization, Supervision, Resources; Writing - Original Draft; Writing - Review &
672 Editing. **Carlotta Bollati:** Investigation, Writing - Original Draft. **Chiara Cavaliere:** Writing -
673 Review & Editing. **Carmela Maria Montone:** Investigation. **Martina Bartolomei:** Investigation.
674 **Giovanna Boschin:** Investigation. **Jianqiang Li:** Investigation. **Susy Piovesana:** Visualization.
675 **Anna Arnoldi:** Writing - Review & Editing. **Aldo Laganà:** Supervision; Project administration

676

677 **Declaration of Competing Interest**

678 The authors declare that they have no known competing financial interests or personal relationships
679 that could have appeared to influence the work reported in this paper.

680 References

- 681 Aguchem, R. N., Okagu, I. U., Okagu, O. D., Ndefo, J. C., & Udenigwe, C. C. (2022). A review on
682 the techno-functional, biological, and health-promoting properties of hempseed-derived
683 proteins and peptides. *Journal of Food Biochemistry*. <https://doi.org/10.1111/jfbc.14127>
- 684 Aiello, G., Lammi, C., Boschin, G., Zanoni, C., & Arnoldi, A. (2017). Exploration of Potentially
685 Bioactive Peptides Generated from the Enzymatic Hydrolysis of Hempseed Proteins. *Journal*
686 *of Agricultural and Food Chemistry*, *65*(47), 10174–10184.
687 <https://doi.org/10.1021/acs.jafc.7b03590>
- 688 Aiello, G., Li, Y., Boschin, G., Bollati, C., Arnoldi, A., & Lammi, C. (2019). Chemical and
689 biological characterization of spirulina protein hydrolysates: Focus on ACE and DPP-IV
690 activities modulation. *Journal of Functional Foods*, *63*, 103592.
691 <https://doi.org/10.1016/j.jff.2019.103592>
- 692 Amigo, L., & Hernández-Ledesma, B. (2020). Current Evidence on the Bioavailability of Food
693 Bioactive Peptides. *Molecules*, *25*(19), 4479. <https://doi.org/10.3390/molecules25194479>
- 694 Bianco, G., Agerbirk, N., Losito, I., & Cataldi, T. R. I. (2014). Acylated glucosinolates with diverse
695 acyl groups investigated by high resolution mass spectrometry and infrared multiphoton
696 dissociation. *Phytochemistry*, *100*, 92–102. <https://doi.org/10.1016/j.phytochem.2014.01.010>
- 697 Bollati, C., Cruz-Chamorro, I., Aiello, G., Li, J., Bartolomei, M., Santos-Sánchez, G., Ranaldi, G.,
698 Ferruzza, S., Sambuy, Y., Arnoldi, A., & Lammi, C. (2022). Investigation of the intestinal
699 trans-epithelial transport and antioxidant activity of two hempseed peptides WVSPLAGRT
700 (H2) and IGFLIIWV (H3). *Food Research International*, *152*, 110720.
701 <https://doi.org/10.1016/j.foodres.2021.110720>
- 702 Boschin, G., Scigliuolo, G. M., Resta, D., & Arnoldi, A. (2014a). ACE-inhibitory activity of
703 enzymatic protein hydrolysates from lupin and other legumes. *Food Chemistry*.
704 <https://doi.org/10.1016/j.foodchem.2013.07.076>
- 705 Boschin, G., Scigliuolo, G. M., Resta, D., & Arnoldi, A. (2014b). Optimization of the enzymatic
706 hydrolysis of lupin (*Lupinus*) proteins for producing ACE-inhibitory peptides. *Journal of*
707 *Agricultural and Food Chemistry*. <https://doi.org/10.1021/jf4039056>
- 708 Brusq, J.-M., Ancellin, N., Grondin, P., Guillard, R., Martin, S., Saintillan, Y., & Issandou, M.
709 (2006). Inhibition of lipid synthesis through activation of AMP kinase: an additional
710 mechanism for the hypolipidemic effects of berberine. *Journal of Lipid Research*, *47*(6), 1281–
711 1288. <https://doi.org/10.1194/jlr.M600020-JLR200>
- 712 Cerrato, A., Aita, S. E., Capriotti, A. L., Cavaliere, C., Montone, C. M., Laganà, A., & Piovesana,
713 S. (2020). A new opening for the tricky untargeted investigation of natural and modified short
714 peptides. *Talanta*, *219*, 121262. <https://doi.org/10.1016/j.talanta.2020.121262>
- 715 Cerrato, A., Capriotti, A. L., Capuano, F., Cavaliere, C., Montone, A. M. I., Montone, C. M.,
716 Piovesana, S., Zenezini Chiozzi, R., & Laganà, A. (2020). Identification and Antimicrobial
717 Activity of Medium-Sized and Short Peptides from Yellowfin Tuna (*Thunnus albacares*)
718 Simulated Gastrointestinal Digestion. *Foods*, *9*(9), 1185. <https://doi.org/10.3390/foods9091185>
- 719 Cruz-Chamorro, I., Santos-Sánchez, G., Bollati, C., Bartolomei, M., Li, J., Arnoldi, A., & Lammi,
720 C. (2022). Hempseed (*Cannabis sativa*) Peptides WVSPLAGRT and IGFLIIWV Exert Anti-
721 inflammatory Activity in the LPS-Stimulated Human Hepatic Cell Line. *Journal of*
722 *Agricultural and Food Chemistry*, *70*(2), 577–583. <https://doi.org/10.1021/acs.jafc.1c07520>
- 723 De Luca, C., Lievore, G., Bozza, D., Buratti, A., Cavazzini, A., Ricci, A., Macis, M., Cabri, W.,
724 Felletti, S., & Catani, M. (2021). Downstream Processing of Therapeutic Peptides by Means of

725 Preparative Liquid Chromatography. *Molecules*, 26(15), 4688.
726 <https://doi.org/10.3390/molecules26154688>

727 Dong, B., Li, H., Singh, A. B., Cao, A., & Liu, J. (2015). Inhibition of PCSK9 Transcription by
728 Berberine Involves Down-regulation of Hepatic HNF1 α Protein Expression through the
729 Ubiquitin-Proteasome Degradation Pathway. *Journal of Biological Chemistry*, 290(7), 4047–
730 4058. <https://doi.org/10.1074/jbc.M114.597229>

731 Ejima, A., Nakamura, M., Suzuki, Y. A., & Sato, K. (2018). Identification of food-derived peptides
732 in human blood after ingestion of corn and wheat gluten hydrolysates. *Journal of Food*
733 *Bioactives*, 2(3), 213–226. <https://doi.org/10.31665/JFB.2018.2145>

734 Farinon, B., Molinari, R., Costantini, L., & Merendino, N. (2020). The Seed of Industrial Hemp
735 (*Cannabis sativa* L.): Nutritional Quality and Potential Functionality for Human Health and
736 Nutrition. *Nutrients*, 12(7), 1935. <https://doi.org/10.3390/nu12071935>

737 Fricker, L. D. (2015). Limitations of Mass Spectrometry-Based Peptidomic Approaches. *Journal of*
738 *the American Society for Mass Spectrometry*, 26(12), 1981–1991.
739 <https://doi.org/10.1007/s13361-015-1231-x>

740 Girgih, A. T., He, R., Malomo, S., Offengenden, M., Wu, J., & Aluko, R. E. (2014). Structural and
741 functional characterization of hemp seed (*Cannabis sativa* L.) protein-derived antioxidant and
742 antihypertensive peptides. *Journal of Functional Foods*, 6, 384–394.
743 <https://doi.org/10.1016/j.jff.2013.11.005>

744 Hertzler, S. R., Lieblein-Boff, J. C., Weiler, M., & Allgeier, C. (2020). Plant Proteins: Assessing
745 Their Nutritional Quality and Effects on Health and Physical Function. *Nutrients*, 12(12),
746 3704. <https://doi.org/10.3390/nu12123704>

747 Iwai, K., Hasegawa, T., Taguchi, Y., Morimatsu, F., Sato, K., Nakamura, Y., Higashi, A., Kido, Y.,
748 Nakabo, Y., & Ohtsuki, K. (2005). Identification of Food-Derived Collagen Peptides in
749 Human Blood after Oral Ingestion of Gelatin Hydrolysates. *Journal of Agricultural and Food*
750 *Chemistry*, 53(16), 6531–6536. <https://doi.org/10.1021/jf050206p>

751 Lammi, C., Aiello, G., Bollati, C., Li, J., Bartolomei, M., Ranaldi, G., Ferruzza, S., Fassi, E. M. A.,
752 Grazioso, G., Sambuy, Y., & Arnoldi, A. (2021). Trans-Epithelial Transport, Metabolism, and
753 Biological Activity Assessment of the Multi-Target Lupin Peptide LILPKHSDAD (P5) and Its
754 Metabolite LPKHSDAD (P5-Met). *Nutrients*, 13(3), 863. <https://doi.org/10.3390/nu13030863>

755 Lammi, C., Aiello, G., Boschini, G., & Arnoldi, A. (2019). Multifunctional peptides for the
756 prevention of cardiovascular disease: A new concept in the area of bioactive food-derived
757 peptides. *Journal of Functional Foods*, 55, 135–145. <https://doi.org/10.1016/j.jff.2019.02.016>

758 Lammi, C., Aiello, G., Dellaflora, L., Bollati, C., Boschini, G., Ranaldi, G., Ferruzza, S., Sambuy,
759 Y., Galaverna, G., & Arnoldi, A. (2020). Assessment of the Multifunctional Behavior of Lupin
760 Peptide P7 and Its Metabolite Using an Integrated Strategy. *Journal of Agricultural and Food*
761 *Chemistry*, 68(46), 13179–13188. <https://doi.org/10.1021/acs.jafc.0c00130>

762 Lammi, C., Aiello, G., Vistoli, G., Zanoni, C., Arnoldi, A., Sambuy, Y., Ferruzza, S., & Ranaldi, G.
763 (2016). A multidisciplinary investigation on the bioavailability and activity of peptides from
764 lupin protein. *Journal of Functional Foods*, 24, 297–306.
765 <https://doi.org/10.1016/j.jff.2016.04.017>

766 Lammi, C., Bollati, C., Gelain, F., Arnoldi, A., & Pugliese, R. (2019). Enhancement of the Stability
767 and Anti-DPP-IV Activity of Hempseed Hydrolysates Through Self-Assembling Peptide-Based
768 Hydrogels. *Frontiers in Chemistry*, 6. <https://doi.org/10.3389/fchem.2018.00670>

769 Li, Y., Aiello, G., Fassi, E. M. A., Boschini, G., Bartolomei, M., Bollati, C., Roda, G., Arnoldi, A.,
770 Grazioso, G., & Lammi, C. (2021). Investigation of *Chlorella pyrenoidosa* Protein as a Source
771 of Novel Angiotensin I-Converting Enzyme (ACE) and Dipeptidyl Peptidase-IV (DPP-IV)
772 Inhibitory Peptides. *Nutrients*, 13(5), 1624. <https://doi.org/10.3390/nu13051624>

773 Lillich, F. F., Imig, J. D., & Proschak, E. (2021). Multi-Target Approaches in Metabolic Syndrome.
774 *Frontiers in Pharmacology*, 11. <https://doi.org/10.3389/fphar.2020.554961>

775 Malomo, S., Onuh, J., Girgih, A., & Aluko, R. (2015). Structural and Antihypertensive Properties

776 of Enzymatic Hemp Seed Protein Hydrolysates. *Nutrients*, 7(9), 7616–7632.
777 <https://doi.org/10.3390/nu7095358>

778 Mazzanti, G., Moro, P. A., Raschi, E., Da Cas, R., & Menniti-Ippolito, F. (2017). Adverse reactions
779 to dietary supplements containing red yeast rice: assessment of cases from the Italian
780 surveillance system. *British Journal of Clinical Pharmacology*, 83(4), 894–908.
781 <https://doi.org/10.1111/bcp.13171>

782 McCarty, M. F., O’Keefe, J. H., & Dinicolantonio, J. J. (2015). Red yeast rice plus berberine:
783 Practical strategy for promoting vascular and metabolic health. In *Alternative Therapies in*
784 *Health and Medicine*.

785 Montone, C. M., Capriotti, A. L., Cavaliere, C., La Barbera, G., Piovesana, S., Zenezini Chiozzi, R.,
786 & Laganà, A. (2018). Characterization of antioxidant and angiotensin-converting enzyme
787 inhibitory peptides derived from cauliflower by-products by multidimensional liquid
788 chromatography and bioinformatics. *Journal of Functional Foods*, 44, 40–47.
789 <https://doi.org/10.1016/j.jff.2018.02.022>

790 Nwachukwu, I. D., & Aluko, R. E. (2021). *CHAPTER 1. Food Protein Structures, Functionality*
791 *and Product Development* (pp. 1–33). <https://doi.org/10.1039/9781839163425-00001>

792 Pérez-Gregorio, R., Soares, S., Mateus, N., & de Freitas, V. (2020). Bioactive Peptides and Dietary
793 Polyphenols: Two Sides of the Same Coin. *Molecules*, 25(15), 3443.
794 <https://doi.org/10.3390/molecules25153443>

795 Piovesana, S., Capriotti, A. L., Cerrato, A., Crescenzi, C., La Barbera, G., Laganà, A., Montone, C.
796 M., & Cavaliere, C. (2019). Graphitized Carbon Black Enrichment and UHPLC-MS/MS
797 Allow to Meet the Challenge of Small Chain Peptidomics in Urine. *Analytical Chemistry*,
798 91(17). <https://doi.org/10.1021/acs.analchem.9b03034>

799 Pontonio, E., Verni, M., Dingo, C., Diaz-de-Cerio, E., Pinto, D., & Rizzello, C. G. (2020). Impact
800 of Enzymatic and Microbial Bioprocessing on Antioxidant Properties of Hemp (*Cannabis*
801 *sativa* L.). *Antioxidants*, 9(12), 1258. <https://doi.org/10.3390/antiox9121258>

802 Röhnert, P., Schmidt, W., Emmerlich, P., Goihl, A., Wrenger, S., Bank, U., Nordhoff, K., Täger,
803 M., Ansorge, S., Reinhold, D., & Striggow, F. (2012). Dipeptidyl peptidase IV,
804 aminopeptidase N and DPPIV/APN-like proteases in cerebral ischemia. *Journal of*
805 *Neuroinflammation*, 9(1), 44. <https://doi.org/10.1186/1742-2094-9-44>

806 Saklayen, M. G. (2018). The Global Epidemic of the Metabolic Syndrome. *Current Hypertension*
807 *Reports*, 20(2), 12. <https://doi.org/10.1007/s11906-018-0812-z>

808 Santini, A., & Novellino, E. (2017). Nutraceuticals in hypercholesterolaemia: an overview. *British*
809 *Journal of Pharmacology*, 174(11), 1450–1463. <https://doi.org/10.1111/bph.13636>

810 Santos-Sánchez, G., Álvarez-López, A. I., Ponce-España, E., Carrillo-Vico, A., Bollati, C.,
811 Bartolomei, M., Lammi, C., & Cruz-Chamorro, I. (2022). Hempseed (*Cannabis sativa*) protein
812 hydrolysates: A valuable source of bioactive peptides with pleiotropic health-promoting
813 effects. *Trends in Food Science & Technology*. <https://doi.org/10.1016/j.tifs.2022.06.005>

814 Segura-Campos, M., Chel-Guerrero, L., Betancur-Ancona, D., & Hernandez-Escalante, V. M.
815 (2011). Bioavailability of Bioactive Peptides. *Food Reviews International*, 27(3), 213–226.
816 <https://doi.org/10.1080/87559129.2011.563395>

817 Strohalm, M., Kavan, D., Novák, P., Volný, M., & Havlíček, V. (2010). mMass 3: A Cross-
818 Platform Software Environment for Precise Analysis of Mass Spectrometric Data. *Analytical*
819 *Chemistry*, 82(11), 4648–4651. <https://doi.org/10.1021/ac100818g>

820 Walker, J. M. (1996). *The Bicinchoninic Acid (BCA) Assay for Protein Quantitation* (pp. 11–14).
821 https://doi.org/10.1007/978-1-60327-259-9_3

822 Wang, B., Xie, N., & Li, B. (2019). Influence of peptide characteristics on their stability, intestinal
823 transport, and in vitro bioavailability: A review. *Journal of Food Biochemistry*, 43(1), e12571.
824 <https://doi.org/10.1111/jfbc.12571>

825 Webb, K. E., Matthews, J. C., & DiRienzo, D. B. (1992). Peptide absorption: a review of current
826 concepts and future perspectives. *Journal of Animal Science*, 70(10), 3248–3257.

827 <https://doi.org/10.2527/1992.70103248x>
828 Wei, L., Dong, Y., Sun, Y., Mei, X., Ma, X., Shi, J., Yang, Q., Ji, Y., Zhang, Z., Sun, H., Sun, X., &
829 Song, S. (2021). Anticancer property of Hemp Bioactive Peptides in Hep3B liver cancer cells
830 through Akt/GSK3 β / β -catenin signaling pathway. *Food Science & Nutrition*, 9(4), 1833–1841.
831 <https://doi.org/10.1002/fsn3.1976>
832 Yuan, R., Yuan, Y., Wang, L., Xin, Q., Wang, Y., Shi, W., Miao, Y., Leng, S. X., Chen, K., &
833 Cong, W. (2022). Red Yeast Rice Preparations Reduce Mortality, Major Cardiovascular
834 Adverse Events, and Risk Factors for Metabolic Syndrome: A Systematic Review and
835 Meta-analysis. *Frontiers in Pharmacology*, 13. <https://doi.org/10.3389/fphar.2022.744928>
836 Zanoni, C., Aiello, G., Arnoldi, A., & Lammi, C. (2017). Hempseed Peptides Exert
837 Hypocholesterolemic Effects with a Statin-Like Mechanism. *Journal of Agricultural and Food*
838 *Chemistry*, 65(40), 8829–8838. <https://doi.org/10.1021/acs.jafc.7b02742>
839
840

841 **FIGURE CAPTIONS**

842
843

844 **Figure 1.** Effect of short-chain peptide mixture (S), medium-chain peptide mixture (M), and total
845 hydrolysate on HMGCoAR activity. Bars represent the mean \pm s.d. of three independent experiments
846 performed in triplicate. *, $p<0.5$; ***, $p<0.001$; ****, $p<0.0001$; ns: not significant

847

848 **Figure 2 A-C:** Modulation of the cholesterol pathway by hempseed peptides. **D:** Effect of hempseed
849 peptides on HepG2 ability to uptake LDL from the extracellular environment. **E,F:** Hempseed
850 peptides modulate the PCSK9 pathway. S: short-chain peptide mixture, M: medium-chain peptide
851 mixture; T: total hydrolysate; MonK: monacolin K. Bars represent the mean \pm s.d. of three
852 independent experiments performed in triplicate. *, $p<0.5$; **, $p<0.001$; ***, $p<0.001$;****,
853 $p<0.0001$; ns: not significant.

854

855 **Figure 3.** Effect of hempseed peptides on DPP-IV activity *in vitro* (A), *in situ* (B), and *ex vivo* (C).
856 S: short-chain peptide mixture, M: medium-chain peptide mixture, and T: total hydrolysate. Bars
857 represent the mean \pm s.d. of three independent experiments performed in triplicate. *, $p<0.5$; ***,
858 $p<0.001$; ***, $p<0.001$;****, $p<0.0001$; ns: not significant

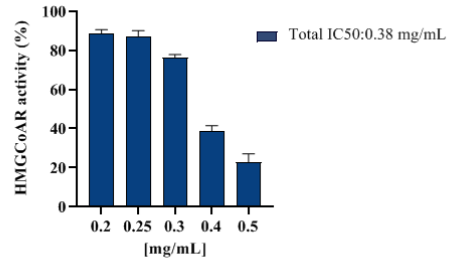
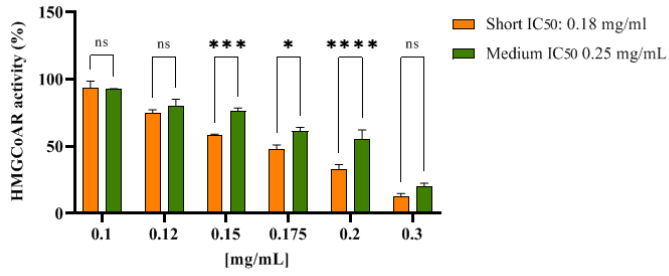
859

860 **Figure 4.** The ACE-inhibitory activity of short- (S) and medium- (M) -chain peptide mixtures and
861 total hydrolysate (T) at 1mg/mL. Bars represent the mean \pm s.d. of three independent experiments
862 performed in triplicate. ****, $p<0.0001$.

863

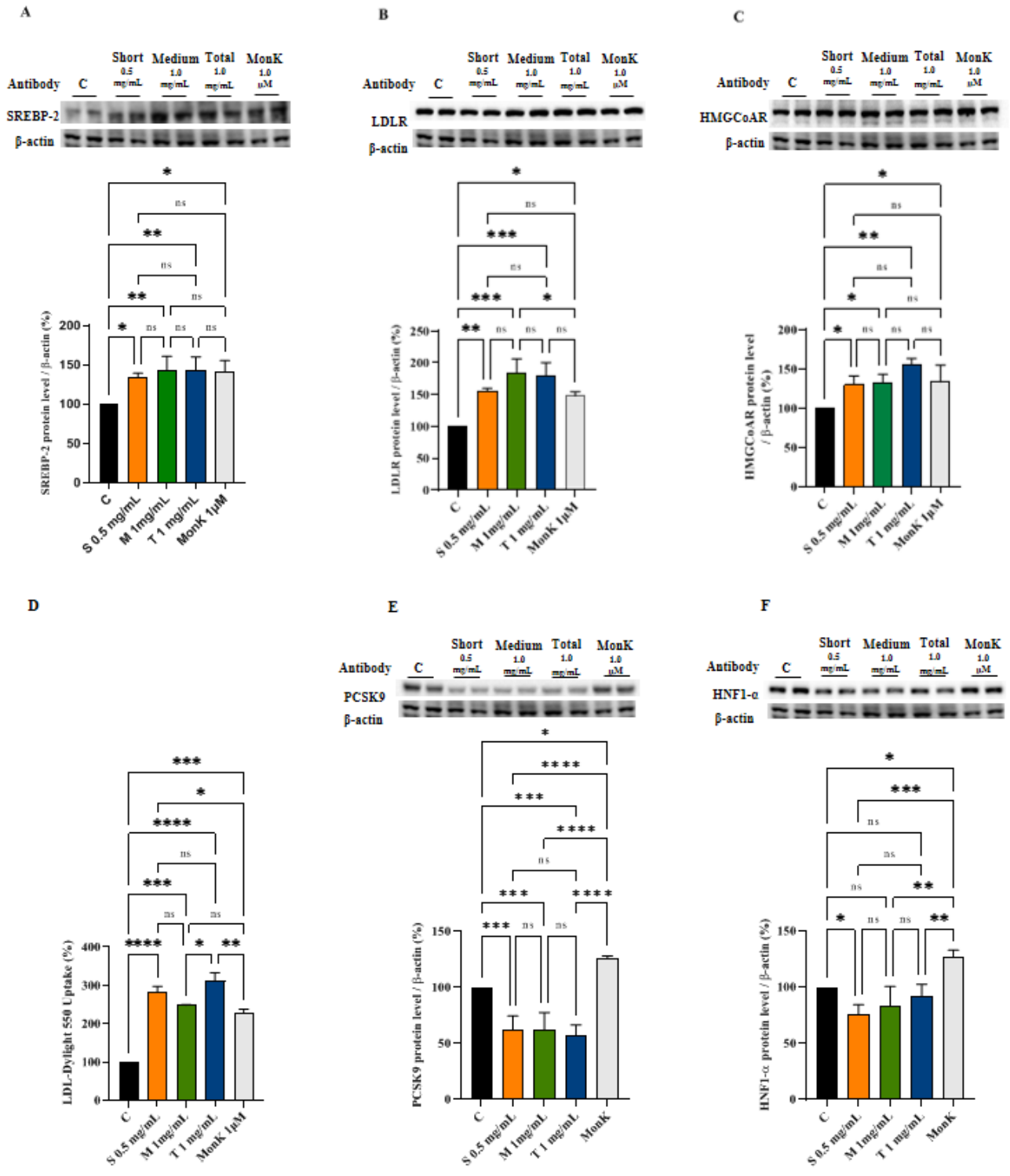
864 **Figure 5.** Direct antioxidant activity of hempseed peptides measured by DPPH (A) and FRAP (B)
865 assays, respectively. S: short-chain peptide mixture, M: medium-chain peptide mixture, and T: total
866 hydrolysate. Bars represent the mean \pm s.d. of three independent experiments performed in triplicate.
867 *, $p<0.5$; ***, $p<0.001$; ***, $p<0.001$;****, $p<0.0001$; ns: not significant

868



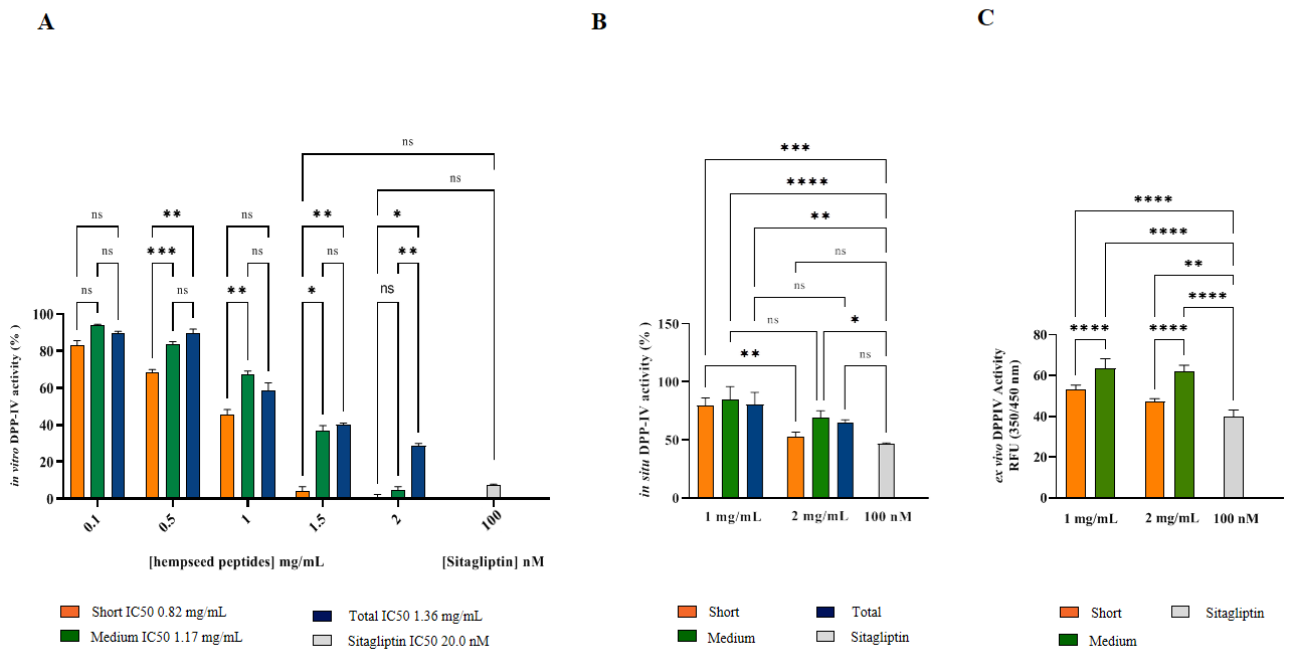
869

870 Figure 1



871

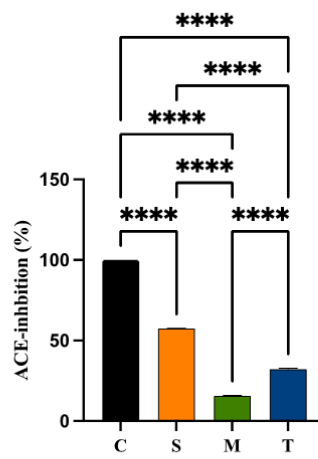
872 Figure 2



873

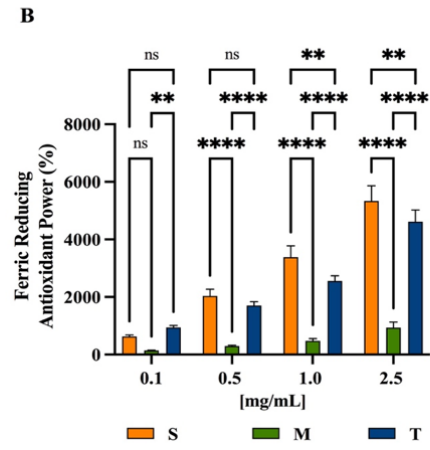
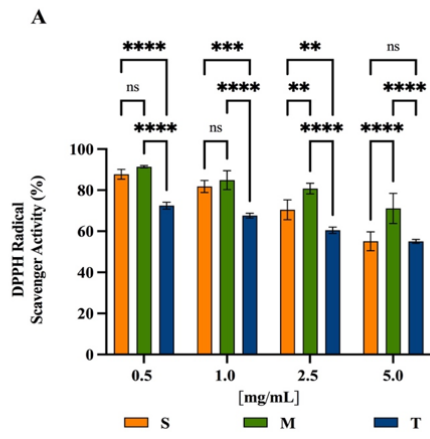
874

875 Figure 3



876

877 Figure 4



878

879

880 Figure 5